

See discussions, stats, and author profiles for this publication at: <https://www.researchgate.net/publication/43297678>

# Calculation of Free-Energy Differences by Confinement Simulations. Application to Peptide Conformers

ARTICLE *in* THE JOURNAL OF PHYSICAL CHEMISTRY B · APRIL 2010

Impact Factor: 3.3 · DOI: 10.1021/jp102878c · Source: PubMed

---

CITATIONS

25

---

READS

20

## 4 AUTHORS, INCLUDING:



**Marco Cecchini**

University of Strasbourg

52 PUBLICATIONS 1,099 CITATIONS

SEE PROFILE



**Martin Spichy**

Ecole normale supérieure de Lyon

31 PUBLICATIONS 684 CITATIONS

SEE PROFILE

## Calculation of Free-Energy Differences by Confinement Simulations. Application to Peptide Conformers

M. Cecchini,<sup>\*,†</sup> S. V. Krivov,<sup>‡</sup> M. Spichty,<sup>†</sup> and M. Karplus<sup>\*,†,§</sup>

Laboratoire de Chimie Biophysique, Université de Strasbourg (ISIS), 8, allée Gaspard Monge, 67000 Strasbourg, France; and Institute of Molecular and Cellular Biology, University of Leeds, Leeds LS2 9JT, U.K.; and Department of Chemistry & Chemical Biology, Harvard University, 12 Oxford Street, Cambridge, Massachusetts 02138

Received: March 6, 2009; Revised Manuscript Received: April 27, 2009

Conformational free-energy differences are key quantities for understanding important phenomena in molecular biology that involve large structural changes of macromolecules. In this paper, an improved version of the confinement approach, which is based on earlier developments, is used to determine the free energy of individual molecular states by progressively restraining the corresponding molecular structures to pure harmonic basins, whose absolute free energy can be computed by normal-mode analysis. The method is used to calculate the free-energy difference between two conformational states of the alanine dipeptide in vacuo, and of the  $\beta$ -hairpin from protein G with an implicit solvation model. In all cases, the confinement results are in excellent agreement with the ones obtained from converged equilibrium molecular dynamics simulations, which have a much larger computational cost. The systematic and statistical errors of the results are evaluated and the origin of the errors is identified. The sensitivity of the calculated free-energy differences to structure-based definitions of the molecular states is discussed. A variant of the method, which closes the thermodynamic cycle by a quasi-harmonic rather than harmonic analysis, is introduced. The latter is proposed for possible use with explicit solvent simulations.

### Introduction

Many proteins and nucleic acids adopt different conformations as part of their function. This flexibility, which is encoded in their structure,<sup>1</sup> has long been recognized as an important aspect of molecular biology. It is involved in enzyme catalysis,<sup>2,3</sup> chemomechanical transduction,<sup>4,5</sup> ion permeation through lipid membranes,<sup>6,7</sup> and allosteric regulation of protein activity,<sup>8,9</sup> among others. The conformational changes are superposed on the dynamic fluctuations of a given conformer, which are implicated in substrate binding and product release, force transmission, molecular translocation, ion gating in biological channels, as well as chemical reactions, which involve inherently dynamic processes since atomic coordinates change along the reaction coordinate. The conformations accessible to a macromolecule interconvert in solution at varying rates depending on the activation free-energy barrier between them.<sup>10,11</sup> Their populations at equilibrium, that is, the probabilities of the macromolecule having a given three-dimensional structure, are determined by the relative free energies of the associated conformational basins. Thus, the calculation of the difference in the free energy for pairs of states provides information on their relative thermodynamic stability and allows the determination of their solution concentrations. Moreover, analysis of the calculation is useful for obtaining insights concerning the factors involved in the stability difference.

Because the computation of the free-energy difference between pairs of conformational states of a macromolecule is a difficult task, there exists no general method for doing so,

particularly for cases where the two conformations differ significantly from each other. Methods such as thermodynamic integration<sup>12</sup> and the exponential formula,<sup>13</sup> which have been increasingly successful in alchemical free-energy simulations,<sup>14,15</sup> are not satisfactory for many conformational problems. If the end states are significantly different, such methods can require a very large computational effort and can suffer from convergence problems (i.e., the so-called “overlap problem”), which may result in sizable errors.<sup>16</sup> To improve the configurational overlap, free-energy calculations are usually divided into multiple steps, termed “windows”, which involve intermediate states along a reaction pathway. The choice of the path is critical for an efficient free-energy estimation because some paths lead to considerably faster convergence than others. This results in one of the classic limitations of free-energy methods, since finding a “good” reaction pathway by projecting the conformational transition on one or more order parameters can be a challenging task.<sup>17</sup> In addition to that, any calculated value of the free-energy difference between two states depends on how they are defined. For alchemical free-energy differences (e.g., changing one amino acid to another), this definition is straightforward. However, for conformational free-energy differences, such as those treated here, the definition is somewhat arbitrary and care is required to select meaningful states.

Given these difficulties, considerable effort is being devoted to the development of efficient conformational free-energy methods for biological systems.<sup>18</sup> Two recent promising developments, the “confinement” approach<sup>19</sup> and the “reference system” method<sup>20</sup> avoid the overlap problem by estimating the absolute free energy of the individual states by introducing a reference state whose free energy is easy to calculate. These methods correspond to the “rediscovery” of techniques introduced a long time ago.<sup>21,24</sup> Other new approaches are “deacti-

\* Corresponding authors. E-mail: mcecchini@isis.u-strasbg.fr (M.C.), marci@tammy.harvard.edu (M.K.).

<sup>†</sup> Université de Strasbourg.

<sup>‡</sup> University of Leeds.

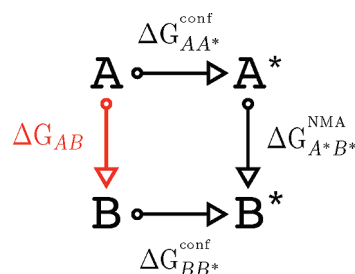
<sup>§</sup> Harvard University.

vated morphing<sup>25</sup> based on the use of a nonphysical path in which the internal molecular interactions are completely turned off during the transformation; the “orthogonal space random walk”<sup>26</sup> which makes use of a random walk in both the reaction coordinate space and its generalized force space to speed-up convergence; and nonequilibrium approaches such as that described in ref 27, which are based on measurements of the work performed during nonequilibrium switches between the investigated states.

In the present paper we focus on the confinement method, which was recently proposed by Tyka et al.<sup>19</sup> The method determines the absolute free energy of the individual states by progressively restraining the molecular conformations to pure harmonic basins, whose absolute free energy can be computed by normal-mode analysis.<sup>28–30</sup> The introduction of the harmonic reference state allows the evaluation of the free-energy change with no need for a direct transformation of one conformational ensemble into the other. We present technical developments that improve the efficiency of the method and show test-case applications on pairs of conformational states of the alanine dipeptide in vacuo, and the  $\beta$ -hairpin from protein G with an implicit solvation model. In both cases, the confinement results are in excellent agreement with the ones obtained from long equilibrium molecular dynamics simulations. The analysis provides an understanding of the possible sources of errors in the confinement calculation and suggests ways to correct for them, which is important for future applications to more complex systems. Also, tests were made of the dependence of the calculated free-energy values on the structure-based definition of molecular states used to extract conformations from the corresponding basins. The confinement results are shown to be robust if the investigated basins are structurally homogeneous. Finally, a variant of the method which closes the thermodynamic cycle by quasi-harmonic analysis is introduced. The latter holds promise for extending the use of the confinement approach to systems with an explicit treatment of the solvent.

Besides the technical aspects, the paper shows the first application of the method to the determination of the free-energy differences between two states of a polypeptide system, i.e., the  $\beta$ -hairpin of protein G. The  $\beta$ -hairpin is an excellent test case: (i) it is a rather flexible system with many degrees of freedom; (ii) it preserves the complexity of the free-energy landscape of a real protein in that there is a well-defined native state along with a denatured state with a large number of nonnative microstates; (iii) it has been characterized in details by computer simulations, so that an exhaustive description of the free-energy basins and barriers among them is available;<sup>31</sup> (iv) its molecular size makes extensive simulations possible and full sampling of the conformational space at equilibrium can be ensured; and (v) its conformational free-energy differences between pairs of states can be computed independently from equilibrium MD and used as a rigorous test of the confinement results. The data presented here indicate that accurate predictions can be obtained at an affordable CPU cost.

The confinement method is reviewed in the next section and the methodological improvements are presented. The free-energy difference between states of the alanine dipeptide and the  $\beta$ -hairpin of protein G, as computed by the improved version of the confinement method, is presented in the third section. The section includes an analysis of the possible sources of errors in the confinement calculation. A discussion of the significance of the results is given in the concluding section.



$$\Delta G_{AB} = \Delta G_{AA^*}^{\text{conf}} - \Delta G_{BB^*}^{\text{conf}} + \Delta G_{A^*B^*}^{\text{NMA}}$$

**Figure 1.** Thermodynamic cycle illustrating the confinement method. **A** and **B** represent molecular conformations corresponding to two different free-energy basins, and **A\*** and **B\*** represent the associated basins harmonically restrained to appropriate reference states. The free energies of confinement for the two molecular states (i.e.,  $\Delta G_{AA^*}^{\text{conf}}$  and  $\Delta G_{BB^*}^{\text{conf}}$ ) are computed by thermodynamic integration. The quantity  $\Delta G_{A^*B^*}^{\text{NMA}}$  is evaluated by normal-mode analysis. The free-energy difference between **A** and **B** conformers,  $\Delta G_{AB}$ , which is the quantity of interest, is obtained by combining the two confinement free energies with  $\Delta G_{A^*B^*}^{\text{NMA}}$  (see equation).

## Material and Methods

**Approach.** The confinement approach to determine the conformational free-energy difference,  $\Delta G_{AB}$ , between two structurally known molecular states (**A** and **B**) is illustrated in Figure 1. The value of  $\Delta G_{AB}$  is obtained by transforming each molecular state into a reference state (**A\*** or **B\***) whose absolute free energy can be computed accurately. Thus, if one can compute the free energy required to transform each actual state to its reference state,  $\Delta G_{AB}$  can be determined without evaluating the transformation between the actual states; the latter could require crossing large energy barriers separating nearly non-overlapping regions of conformational space. The key to the efficiency of the method is to choose reference states that are strongly overlapping with the actual states, so that the free-energy difference can be efficiently computed by using standard methods such as thermodynamic integration<sup>12</sup> or the exponential formula.<sup>13</sup> In the confinement method, the reference state is chosen to be a pure harmonic state for which the absolute free energy can be computed analytically by normal-mode or quasi-harmonic analyses, which yield identical results. Starting from each of the two molecular states, the system is transformed into the corresponding reference by introducing a harmonic potential with an increasing force constant. During the confinement, the conformational space available to the system is progressively reduced and the work performed by the restraining potential is recorded. The latter corresponds to the free-energy cost of reducing all nonharmonic contributions to the  $\Delta G$  between the initial (anharmonic) and final (harmonic) states to a negligible value relative to the harmonic term, which can be calculated exactly; it is hereafter referred to as the free energy of confinement. In this analysis, the confinement free energies were computed by thermodynamic integration (see Methods). The normal-mode or quasi-harmonic free-energy change between the harmonically restrained states was then applied to close the thermodynamic cycle.

**Theory. Conformational Free-Energy Difference.** The free-energy difference between the molecular states **A** and **B** is obtained from the thermodynamic cycle depicted in Figure 1. The calculation is performed as follows. First, a reference state for each free-energy basin is selected. Then, a series of confinement simulations are performed with increasing restraint strengths ( $k$ ) until the harmonic potential is sufficiently strong that the normal-mode approximation applies well. For each

simulation, the ensemble-averaged atomic deviations from the reference are computed as a function of  $k$  by measuring the average rmsd. These data are numerically integrated to compute the confinement free energy for each molecular state, i.e.,  $\Delta G_{AA^*}^{\text{conf}}$  and  $\Delta G_{BB^*}^{\text{conf}}$ . At the final restraint strength ( $k = k_f$ ) a normal-mode analysis is performed and the vibrational free-energy difference between the confined states ( $A^*$  and  $B^*$ ) is computed through the canonical partition function of the classic harmonic oscillator. By combining the two confinements with the normal-mode analysis one obtains the desired free-energy difference

$$\Delta G_{AB} = \Delta G_{AA^*}^{\text{conf}} - \Delta G_{BB^*}^{\text{conf}} + \Delta G_{A^*B^*}^{\text{NMA}} \quad (1)$$

where  $\Delta G_{AA^*}^{\text{conf}} = G_{A^*} - G_A$ ,  $\Delta G_{BB^*}^{\text{conf}} = G_{B^*} - G_B$ , and  $\Delta G_{A^*B^*}^{\text{NMA}} = G_{B^*} - G_{A^*}$ . Each confinement simulation measures the anharmonic contribution of a given molecular state to the overall free-energy difference  $\Delta G_{AB}$ , which is not included in the normal-mode calculation. The confinement free-energy is related to the entropic cost associated with the restriction of the conformational space accessible to the system in a harmonic model. However, it does not coincide with the difference in conformational entropy between the states under study. Perhaps surprisingly and in disagreement with a previous suggestion,<sup>25</sup> an analysis of the thermodynamic components of  $\Delta G^{\text{conf}}$  for the alanine dipeptide indicates that the enthalpic and entropic contributions to the confinement free-energy difference are comparable in magnitude (see Supporting Information). The calculation of each contribution to the conformational free-energy difference (eq 1) is described in turn.

**Confinement Simulations.** Thermodynamic integration<sup>12,32</sup> expresses the difference in free energy between two states as

$$\Delta G = \int_0^1 \langle \partial U(\mathbf{X}, \lambda) / \partial \lambda \rangle_\lambda d\lambda \quad (2)$$

where  $\lambda$  is a dimensionless parameter defining the integration path running from 0 to 1,  $\partial U(\mathbf{X}, \lambda) / \partial \lambda$  is the derivative of the potential energy with respect to  $\lambda$ , and  $\langle \dots \rangle$  indicates an ensemble average at a particular  $\lambda$ . This integration is usually performed numerically by recording individual values of  $\partial U(\mathbf{X}, \lambda) / \partial \lambda$  and using the trapezoidal or Simpson's rule.

To calculate the confinement free energy, i.e.,  $\Delta G_{AA^*}^{\text{conf}}$  and  $\Delta G_{BB^*}^{\text{conf}}$  in Figure 1, one needs to perturb the free system A at  $\lambda = 0$  to the restrained system A\* at  $\lambda = 1$ . The energy function  $U(\mathbf{X}, \lambda)$  is thus

$$U(\mathbf{X}, \lambda) = U_{\text{ff}}(\mathbf{X}) + \frac{1}{2} \lambda k_f |\mathbf{X} - \mathbf{X}_0|^2 \quad (3)$$

where  $U_{\text{ff}}(\mathbf{X})$  is the energy of the system with coordinate  $\mathbf{X}$  calculated from the force field,  $\mathbf{X}$  is the vector of atomic positions,  $\mathbf{X}_0$  is the configuration of the reference structure, and  $k_f$  is the final restraint force constant at  $\lambda = 1$ . The second term of eq 3 is the harmonic potential that is used to confine the system. In principle, any type of restraint is suitable provided that it is sufficiently tight at  $\lambda = 1$  such that the normal-mode approximation is accurate. Here, we chose a harmonic restraint which is similar in nature to the absolute Cartesian restraint adopted in ref 19 except that the atomic coordinates of the reference are implicitly rotated and translated so as to best fit the atoms of the actual molecular frame. The newly adopted restraining potential, which projects out the contributions to the confinement free energy resulting from the translational and rotational modes, has the advantage that it

minimizes the total restraint energy and does not introduce any net force or torque on the system.

If one introduces  $k = \lambda k_f$ , eq 2 can be restated using  $k$  as the variable of integration instead of  $\lambda$  as

$$\Delta G^{\text{conf}} = \frac{1}{2} \int_0^{k_f} \langle |\mathbf{X} - \mathbf{X}_0|^2 \rangle_k dk = \frac{1}{2} \int_0^{k_f} X_k dk \quad (4)$$

where

$$X_k = \langle |\mathbf{X} - \mathbf{X}_0|^2 \rangle_k \quad (5)$$

It follows from eqs 4 and 5 that the free energy of confinement can be obtained by simply recording the ensemble averages of the atomic deviations from the reference structure at different restraint strengths,  $k$ , and performing numerical integration over these values.

**Fluctuations from the Reference Structure.** The most obvious way to compute the ensemble-averaged  $X_k$  (eq 5) consists in recording the time series of the restraint energy at different values of  $k$ . From eq 3 it follows that

$$U_{\text{cons}} = \frac{1}{2} \lambda k_f |\mathbf{X} - \mathbf{X}_0|^2 \quad (6)$$

Thus, by introducing  $k$

$$\frac{2U_{\text{cons}}}{k} = |\mathbf{X} - \mathbf{X}_0|^2 \quad (7)$$

and computing the ensemble average

$$X_k = \frac{2\langle U_{\text{cons}} \rangle_k}{k} \quad (8)$$

that is an operational definition of  $X_k$ .<sup>19</sup> However, this definition does not allow computation of  $X_k$  for the free system (i.e.,  $k$  equal to zero) and is expected to suffer from numeric instability as vanishing  $k$  is approached. Alternatively,  $X_k$  can be deduced from the all-atom root-mean-square deviation (rmsd) from the reference structure  $\mathbf{X}_0$ . In fact, from eq 5 and the definition of the ensemble average one can write that

$$X_k = \frac{1}{M} \sum_{j=1}^M (\mathbf{X}_j^k - \mathbf{X}_0)^2 \quad (9)$$

where  $j$  runs over the  $M$  molecular snapshots sampled in the simulation in the presence of the restraining potential with force constant  $k$ . Given that the rmsd from the reference of the  $j$ th molecular conformation is

$$\text{RMSD}_j = \sqrt{\frac{1}{N} (\mathbf{X}_j^k - \mathbf{X}_0)^2} \quad (10)$$

where  $N$  the total number of atoms in the molecule, it follows that

$$N \cdot \text{RMSD}_j^2 = (\mathbf{X}_j^k - \mathbf{X}_0)^2 \quad (11)$$



Thus, by computing the average over the canonical ensemble and combining the result with eqs 5 and 9, one obtains

$$X_k = \langle N \cdot \text{RMSD}^2 \rangle_k \quad (12)$$

which states that the atomic fluctuations  $X_k$  can be computed from the ensemble average of the rmsd from the reference structure for each value of the integration variable  $k$ . The new definition for  $X_k$  is more robust than the one given by eq 8. In fact, since the average rmsd has always a finite value even for the free (unrestrained) system, eq 12 does not diverge for vanishing  $k$ . In this study, eq 12 was used to compute the free energy of confinement.

**Numerical Integration.** The integration scheme proposed by Tyka et al.<sup>19</sup> was applied to compute the free energy of confinement. Numerical integration of the atomic fluctuations from the reference was performed by using the trapezoidal rule in a double log scale and fitting between successive data points with a power law of the form

$$X_k = ak^b \quad (13)$$

For two successive data points  $P_i = (X_{k_i}, k_i)$  and  $P_j = (X_{k_j}, k_j)$  with  $j = i + 1$ , the area  $L_j$  underneath the fitted curve is given by

$$L_j = \int_{k_i}^{k_j} ak^b dk = \frac{a}{b+1} [k^{b+1}]_i^j = \frac{a}{b+1} [k^b k]_i^j \quad (14)$$

and by substituting eq 13 into eq 14, one obtains

$$L_j = \frac{1}{b+1} [X_k k]_i^j = \frac{1}{b+1} (X_{k_j} k_j - X_{k_i} k_i) \quad (15)$$

where  $b$  is obtained from eq 13 by introducing  $\ln X_k$ ,

$$\begin{aligned} \ln X_{k_j} &= \ln a + b \ln k_j \\ \ln X_{k_i} &= \ln a + b \ln k_i \end{aligned} \quad (16)$$

and subtracting the second equation from the first. [We note that in the original confinement paper the area underneath two successive data points is defined by a two-parameter expression (see eqs 4–6 in ref 19). The simple mathematical manipulation introduced in eq 15 allows one to simplify the expression such that it becomes dependent on a single parameter,  $b$ . Also, we note that eq 6 in ref 19 is mistyped and should be written as eq 17.] That is

$$b = \frac{\ln X_{k_j} - \ln X_{k_i}}{\ln k_j - \ln k_i} \quad (17)$$

The confinement free-energy change between states A and A\* is given by

$$\Delta G_{AA^*}^{\text{conf}} = \sum_j L_j \quad (18)$$

**Normal-Mode Analysis (NMA).** The absolute free energy of the restrained conformations (A\* or B\*) is calculated using the classical formula for the canonical partition function of a system of  $N$  particles with  $\kappa$  vibrational degrees of freedom<sup>33</sup>

$$Z = \exp(-E_0/k_B T) \prod_i^{\kappa} \frac{k_B T}{h \nu_i} \quad (19)$$

where  $\nu_i$  is the frequency of the  $i$ th normal mode,  $E_0$  is the potential energy at the minimum,  $T$  is the temperature,  $h$  is Planck's constant, and  $k_B$  is the Boltzmann constant. Knowledge of the partition function enables one to calculate the free energy of the restrained state ( $G_{A^*}$ ) by

$$G_{A^*} = -k_B T \ln Z_A \quad (20)$$

Thus, the remaining leg of the thermodynamic cycle shown in Figure 1 is computed directly (without the need to construct a path to transform A into B) as

$$\Delta G_{A^*B^*}^{\text{NMA}} = G_{B^*} - G_{A^*} \quad (21)$$

The normal-mode frequencies, which are used to compute  $\Delta G_{A^*B^*}^{\text{NMA}}$  by solving eqs 19 and 20, are obtained by finding the eigenvalues of the mass-weighted matrix of second derivatives of the effective energy (Hessian) at the minimum. For this purpose, the reference structure was energy-minimized in the presence of the full restraining potential (i.e.,  $k = k_f$ ) by performing 5000 SD steps followed by 10000 additional ABNR steps; we note that if a well energy-minimized conformation is used as reference, energy minimization in the presence of the restraining potential has no effect on the structure (see Figure S9 in the Supporting Information). Normal-mode analysis on the resulting structure in the all-atom representation was performed by using the VIBRAN module in CHARMM.<sup>34</sup> Since a *best-fit* restraint is applied to confine the system, only the  $3N - 6$  nonzero frequencies corresponding to the internal degrees of freedom are included in calculating  $G_{A^*}$  (or  $G_{B^*}$ ). We note that a quantum mechanical analysis of the vibrational free-energy difference between the harmonically restrained states yields essentially the same result as the classical analysis (see Supporting Information for details).

**Quasi-Harmonic Analysis (QHA).** Alternatively, the absolute free energy of the restrained conformations (A\* or B\*) can be calculated by a quasi-harmonic analysis. In the quasi-harmonic approximation the fluctuations observed during the motions of the system are described by a multivariate Gaussian probability distribution.<sup>35</sup> Under this assumption, a temperature-dependent effective potential of a quadratic form, which results in the Gaussian probability distribution, can be defined<sup>36</sup> and the quasi-harmonic modes computed from the mass-weighted Hessian defined in terms of its elements as  $F_{ij} = k_B T (\sigma^{-1})_{ij}$ . The  $F_{ij}$  are computed from the temperature-dependent variances (diagonal elements) and covariances (off-diagonal elements) of the Cartesian coordinates fluctuations,

$$\sigma_{ij} = \langle (x_i - \bar{x}_i)(x_j - \bar{x}_j) \rangle \quad (22)$$

which are obtained from a molecular dynamics simulation. Thus, by solving the secular equation

$$\det(\mathbf{F} - \omega^2 \mathbf{M}) = \det\left(\mathbf{M}^{1/2} \sigma \mathbf{M}^{1/2} - \frac{kT}{\omega^2} \mathbf{1}\right) = 0 \quad (23)$$

where  $\mathbf{M}$  is the mass matrix, one obtains the quasi-harmonic frequencies  $\omega_k$ , which are used to compute the vibrational entropy in the classical expression

$$S^{\text{QHA}} = k_B \sum_{k=1}^{3N-6} \ln\left(\frac{k_B T}{h \omega_k}\right) \quad (24)$$

where  $k_B$  is the Boltzmann constant,  $T$  the temperature,  $h$  is the Planck's constant, and  $\omega_k$  the  $k$ th quasi-harmonic frequency. Finally, the quasi-harmonic free energy is obtained as

$$G^{\text{QHA}} = H^{\text{QHA}} - TS^{\text{QHA}} \quad (25)$$

where  $H^{\text{QHA}}$  is the ensemble-averaged effective energy determined from the MD run.

In the confinement calculation, the quasi-harmonic analysis is applied to the MD run carried out in the presence of the strongest restraining potential ( $k = k_f$ ) for each molecular state. Note that at large restraint strengths, the harmonic approximation holds and the quasi-harmonic result for the free energy is correct. Although the answers from QHA and NMA must be identical in the limit of the harmonic approximation, the former enables the analysis of a subset of degrees of freedom of the system, thus opening the possibility of using the confinement approach in the context of explicit solvent simulations (see Discussion).

**Free-Energy Profiles.** One-dimensional barrier preserving free-energy profiles provide a rigorous yet intuitive description of the system kinetics.<sup>37,38</sup> Here, cut-based free-energy profiles projected onto the “natural coordinate”,<sup>39</sup> which is constructed such that the diffusion coefficient is constant along the profile, were computed for various restrained runs and used to examine the origin of statistical errors in the confinement calculation (see Results). For this purpose, the MD simulations were first projected onto the principal component space defined by the distance between all atom pairs.<sup>40</sup> This space is defined by the eigenvectors of the covariance matrix of the interatomic distances. Molecular snapshots sampled by MD were then clustered by binning the first three principal components so as to build an equilibrium kinetic network in which nodes and links, respectively, correspond to molecular configurations and directed transitions between pairs of nodes.<sup>41</sup> Finally, the free-energy profiles were computed by the “pfoldf” method described in ref 37. The resulting profile is invariant with respect to any arbitrary transformation of the reaction coordinate and is plotted as a function of the “natural coordinate”.<sup>39</sup>

**Systems and Setups.** The molecular systems used for this study are the alanine dipeptide and the  $\beta$ -hairpin from protein G. The alanine dipeptide is the *N*-acetyl-*N'*-methylamide derivative of alanine, which has become a standard model for theoretical studies.<sup>27,42–46</sup> The  $\beta$ -hairpin from protein G is a 16-residue peptide that has been shown by NMR to fold even in the absence of the rest of the protein.<sup>47</sup> The  $\beta$ -hairpin peptide, which has the following amino-acid sequence Gly-Glu-Trp-Thr-Tyr-Asp-Asp-Ala-Thr-Lys-Thr-Phe-Thr-Val-Thr-Glu, is an interesting system because in spite of the small size it preserves the complexity of the free-energy landscape of a real protein.<sup>31</sup>

**Alanine Dipeptide.** The alanine dipeptide was modeled with the polar-hydrogen potential function (12 atoms)<sup>48</sup> and simulated

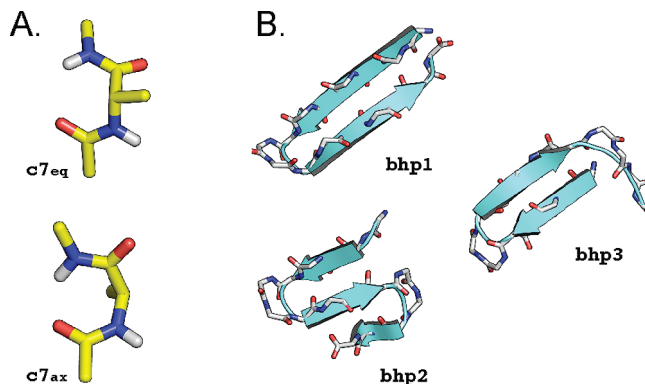


**Figure 2.** Molecular systems and conformational states used for this study. (A) Alanine dipeptide. The **c7eq** and **c7ax** molecular structures were considered; they correspond to the deepest free-energy basins at 300 K in vacuo (see Figure S1 in Supporting Information). (B)  $\beta$ -Hairpin from protein G. Three molecular states were investigated: the native  $\beta$ -hairpin state (**bhp1**), the three-stranded  $\beta$ -sheet state (**bhp2**), and an out-of-register  $\beta$ -hairpin state (**bhp3**); they were previously identified as representative of the three deepest free-energy basins at 360 K.<sup>31</sup> Molecular representations were drawn with the help of PYMOL.<sup>55</sup>

in vacuo at 300 K with infinite cutoffs for the nonbonded interactions. The system was simulated in vacuo because the corresponding free-energy landscape includes only two significant minima (**c7eq** and **c7ax**, see Figure S1, Supporting Information) which are separated by high free-energy barriers (8.5 and 10.5 kcal/mol from **c7eq**),<sup>49</sup> i.e., it results in a simplified energy landscape and introduces a challenging task for the determination of the free-energy difference between the states of interest due to the large barriers between them. For all MD simulations, Langevin dynamics with a friction value of  $1.0 \text{ ps}^{-1}$  was used; the friction is introduced to enhance the Markovian character of the time evolution of the system so as to improve the sampling efficiency, including energy transfer among the normal modes. The integration time step was set to 1 fs. Such setup ensures that molecular configurations saved every 1000 steps (1 ps) are independent. Two conformational states, called **c7eq** and **c7ax**, were considered (see Figure 2A).

**$\beta$ -Hairpin from Protein G.** The  $\beta$ -hairpin peptide was modeled with the polar-hydrogen potential function<sup>48</sup> with no blocking groups for the terminal residues (160 atoms). Solvation effects were approximated by the EEF1 model<sup>50</sup> which contains screened electrostatic interactions and a Gaussian term to represent the hydrophobic interactions. This model was used to permit comparison with earlier work.<sup>31</sup> Accordingly, MD simulations were carried out at 360 K. Langevin dynamics with a friction value of  $1.0 \text{ ps}^{-1}$  was used for all runs to increase sampling efficiency; although such friction is much smaller than the one of water (i.e.,  $28 \text{ ps}^{-1}$  at 360 K), the thermodynamic properties of the system are, of course, independent of the friction used. The SHAKE algorithm<sup>51</sup> was used to fix the length of the covalent bonds involving hydrogen atoms, which allows for an integration time step of 2 fs. Molecular snapshots were saved every 1000 steps (2 ps). Three conformational states were considered: the native  $\beta$ -hairpin state (**bhp1**), the three-stranded  $\beta$ -sheet state (**bhp2**), and an out-of-register  $\beta$ -hairpin state (**bhp3**); see Figure 2B. These structures were identified in a previous MD simulation study<sup>31</sup> as representative of the three deepest free-energy basins at 360 K.

**Confinement Simulation Setup.** A confinement simulation requires introduction of a number of parameters. The choice for these parameters is not trivial and may be system dependent. They include the following: (i) the range of restraint strength

to be investigated (i.e.,  $k_{\min}$  and  $k_{\max}$ ); (ii) the distribution of the restraint strengths in that range; (iii) the number of restrained runs to be performed; (iv) the length of the individual MD runs; (v) the selection of the reference state; and (vi) the structural definition of the free-energy basins corresponding to the molecular states under investigation. The results presented in this paper indicate that it is possible to rationalize the choice of (ii) and (v), while the remaining parameters have to be justified by examining the convergence of the results. Consequently, the parameters for the two systems are given in the corresponding result sections (see below). All restrained MD runs were performed with the program CHARMM.<sup>34</sup> Efficient analysis of the simulations was performed with the program Wordom;<sup>52</sup> the latter was used to identify molecular snapshots belonging to the basins of interest and compute the ensemble-averaged fluctuations from the time series of the all-atom rmsd from the reference structure.

## Results

**Alanine Dipeptide in Vacuo.** The confinement approach is applied to compute  $\Delta G_{AB}$  between the **c7eq** and **c7ax** conformational states of the alanine dipeptide in vacuo (Figure 2A). For the confinement in each minimum, 23 restrained MD simulations with harmonic force constants ranging from  $1.95 \times 10^{-5}$  to  $82 \text{ kcal/mol/Å}^2$  were performed; intermediate  $k$  values are determined from the recursive sequence  $k_i = 2k_{i-1}$ , with  $k_0 = 1.95 \times 10^{-5} \text{ kcal/mol/Å}^2$ . Each MD run was carried out for 20 ns independent of the restraint strength, which corresponds to 20000 molecular frames per run at a saving frequency of 1 configuration/ps. Thus, the total simulation time is 920 ns per confinement calculation (i.e., 23 runs  $\times$  20 ns  $\times$  2 legs). Deeply energy-minimized conformations were selected as reference structures for each molecular state. The value of the  $\varphi$  dihedral angle was used to assign molecular configurations sampled by MD to the **c7eq** or **c7ax** free-energy basins; i.e., given the simple shape of the free-energy surface in vacuo, structures with  $0 \leq \varphi \leq 130$  were assigned to the **c7ax** basin and the others to **c7eq** (see Figure S1 in Supporting Information for details). The time series of the all-atom rmsd from the reference structure were collected for each restrained run and used to compute the ensemble-averaged atomic fluctuations,  $X_k$ . Numerical integration of these data points with  $k_f$  equal to  $82 \text{ kcal/mol/Å}^2$  yielded confinement free energies of 8.04 and  $7.25 \text{ kcal/mol}$  for **c7eq** and **c7ax**, respectively (see Figure 3A). NMA on the reference structures minimized in the presence of the largest restraining potential provided a  $\Delta G^{\text{NMA}}$  of  $2.11 \text{ kcal/mol}$  ( $\Delta H^{\text{NMA}}$  and  $T\Delta S^{\text{NMA}}$  are equal to  $2.00$  and  $-0.11 \text{ kcal/mol}$ , respectively); see Figure 3B. As described by eq 1, the confinement calculation with  $k_f$  equal to  $82 \text{ kcal/mol/Å}^2$  yielded a  $\Delta G_{AB}$  of  $2.90 \pm 0.02 \text{ kcal/mol}$  between **c7eq** and **c7ax** in vacuo (Figure 3C); the free-energy error was approximated by means of the specialized block analysis presented below. This value is in good agreement with the free-energy difference at 300 K obtained from a  $6 \mu\text{s}$  replica-exchange molecular dynamics<sup>53</sup> simulation ( $3.02 \pm 0.13 \text{ kcal/mol}$ ), and  $2.5$  ( $2.96 \pm 0.11 \text{ kcal/mol}$ ) and  $4.2 \mu\text{s}$  ( $2.92 \pm 0.03 \text{ kcal/mol}$ ) equilibrium MD sampling at 400 and 500 K after Boltzmann reweighting (see Supporting Information for details);  $\Delta G_{AB}$  values obtained from these calculations are given in parentheses. We observe that while the individual contributions on the right-hand side of eq 1 keep changing as a function of  $k_f$ , the conformational  $\Delta G$  has converged for  $k_f$  larger than  $2 \text{ kcal/mol/Å}^2$  (Figure 3C).

The analysis was repeated by using a variant of the confinement method that applies a quasi-harmonic analysis (QHA) to

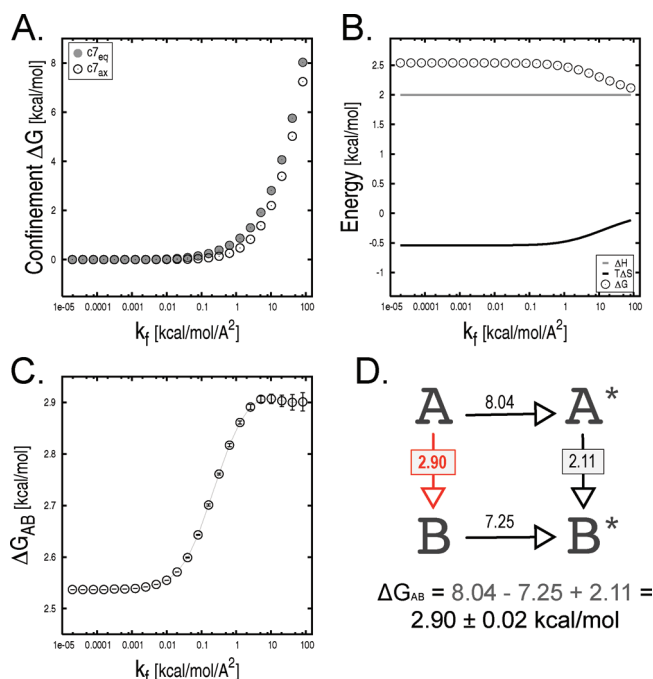


**Figure 3.** Confinement analysis of the **c7eq** and **c7ax** states of the alanine dipeptide in vacuo. All free-energy terms are shown as a function of the final restraint strength,  $k_f$ . (A) Confinement free energies for both molecular states. (B) Harmonic free-energy difference; both the enthalpic and entropic harmonic contributions are shown. (C) Total free-energy difference (i.e.,  $\Delta G_{c7ax} - \Delta G_{c7eq}$ ) with the associated error. For  $k_f$  larger than  $2 \text{ kcal/mol/Å}^2$ ,  $\Delta G_{AB}$  has converged to a value of  $2.90 \pm 0.02 \text{ kcal/mol}$ . (D) Thermodynamic analysis corresponding to a final restraint strength of  $82 \text{ kcal/mol/Å}^2$ . Molecular states **A** and **B** correspond to **c7eq** and **c7ax**, respectively.

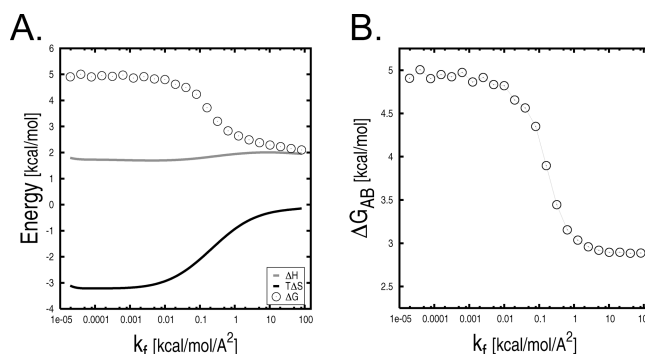


**Figure 4.** Confinement analysis of the **c7eq** and **c7ax** states of the alanine dipeptide in vacuo by the quasi-harmonic variant. (A) Quasi-harmonic free-energy difference as a function of  $k_f$ ; both the enthalpic and entropic harmonic contributions are shown. (B) Total free-energy difference (i.e.,  $\Delta G_{c7ax} - \Delta G_{c7eq}$ ) as a function of  $k_f$ .

compute the free-energy change between the harmonically restrained states. The QHA results are reported in Figure 4A as a function of  $k_f$ . At the strongest restraining potential (i.e.,  $k_f = 82 \text{ kcal/mol/Å}^2$ )  $\Delta G_{A \rightarrow B^*}$  is equal to  $2.10 \text{ kcal/mol}$ , which is in excellent agreement with the value obtained from NMA (see above). By solving eq 1, the quasi-harmonic variant of the confinement method gives a free-energy change of  $2.90 \text{ kcal/mol}$ . In analogy to the above, this value has converged for  $k_f$  larger than  $2 \text{ kcal/mol/Å}^2$  (Figure 4B). We note that the quasi-harmonic variant of the confinement method approaches the correct  $\Delta G_{AB}$  from the above, whereas the normal-mode variant does it from below (cfr Figure 3C with Figure 4B).

**$\beta$ -Hairpin from Protein G.** The confinement approach was applied to compute the free-energy difference between basins



1 and 2 of the  $\beta$ -hairpin peptide (see Figure 2B). For the confinement in each minimum, 23 restrained MD simulations with harmonic force constants ranging from  $1.95 \times 10^{-5}$  to 82 kcal/mol/Å<sup>2</sup> were performed; i.e., the setup for the confinement experiment is essentially the same as for the alanine dipeptide. The system was simulated for 100 ns at each restraint strengths, which corresponds to 50000 molecular frames per run for a total sampling of 4.6  $\mu$ s per confinement simulation (i.e., 23 runs  $\times$  100 ns  $\times$  2 legs). The centers of the most-populated clusters at 360 K were chosen as the reference structures for **bhp1** and **bhp2**; they were found by equilibrium MD simulations at 360 K.<sup>31</sup> Molecular conformations belonging to the respective basins were extracted from the restrained MD runs. Given that an a priori definition for a free-energy basin does not exist, a  $C_{\alpha}$ -rmsd of 2.0 Å from the reference structure was arbitrarily chosen as a criterion to define the boundaries of the basin and filter out “noncontributing” conformations, i.e., conformations sampled by MD but considered to be part of other basins (see also below). The time series of the all-atom rmsd from the reference were collected and used to compute the ensemble-averaged atomic fluctuations,  $X_k$ . The distribution of the rmsd is relatively broad for low restraint strengths (i.e.,  $k < 1.00 \times 10^{-2}$  kcal/mol/Å<sup>2</sup>), and it becomes much more “peaked” when large force constants are applied (see Figure S8 in Supporting Information). Accordingly,  $X_k$  values converge rapidly in the high  $k$  range, whereas longer simulations are required in the low  $k$  range. In the case of  $\beta$ -hairpin, convergence in  $X_k$  is rapid in the whole  $k$  range; i.e., on the order of a few nanoseconds for  $k > 1.00 \times 10^{-2}$  and dozens of nanoseconds for  $k < 1.00 \times 10^{-2}$  (see Figure S8 in Supporting Information).  $X_k$  values at different restraint strengths are shown in Figure 5A (top). Numerical integration of the data points with  $k_f$  equal to 82 kcal/mol/Å<sup>2</sup> yields confinement free energies of 301.11 and 317.73 kcal/mol for **bhp1** and **bhp2**, respectively. NMA on the reference structures minimized by 5000 steps of SD followed by 10000 steps of ABNR in the presence of a restraining potential with a spring constant of 82 kcal/mol/Å<sup>2</sup> yields a  $\Delta G_{A^*B^*}$  of 18.05 kcal/mol ( $\Delta H^{NMA}$  and  $T\Delta S^{NMA}$  are equal to 17.54 and  $-0.51$  kcal/mol, respectively); see Figure 5A, middle. The  $\Delta G_{AB}$  is determined by solving eq 1. Figure 5A (bottom) shows the value of  $\Delta G_{AB}$  as a function of  $k_f$ . When the harmonic approximation applies well (i.e.,  $k > 20$  kcal/mol/Å<sup>2</sup>) similar free-energy difference are obtained. For  $k_f$  equal to 82 kcal/mol/Å<sup>2</sup> the confinement calculation yields a  $\Delta G_{AB}$  (i.e.,  $\Delta G_{bhp2} - \Delta G_{bhp1}$ ) of 1.42 kcal/mol.

**Selection of the Reference State.** The free-energy difference between the *confined* states,  $\Delta G_{A^*B^*}^{NMA}$ , strongly depends on the value of  $k$  (Figure 5A, middle). For increasing  $k$ ,  $\Delta G^{NMA}$  increases monotonically until it plateaus at very large restraining strengths ( $k > 10^4$  kcal/mol/Å<sup>2</sup>, data not shown). By considering the different contributions to the free-energy change, it is apparent that the enthalpic term (in gray) dominates over the entropic one (in black). The reason for such a behavior lies in the choice of the reference structure for the confinement simulations, which appears not to be appropriate. In fact, a cluster center is a relatively high potential energy conformation which does not correspond to a minimum on the potential energy surface (PES). Thus, during the confinement the restraining potential not only reduces the conformational space available to the molecule but performs work against the molecular potential. The latter has important consequences: (i) the enthalpic contribution to  $\Delta G^{NMA}$  is largely dominant, thus making NMA essentially useless; (ii) much larger restraint strengths are required to stabilize the enthalpic term in the NMA leg, thus increasing the number of restrained MD runs required; (iii) the

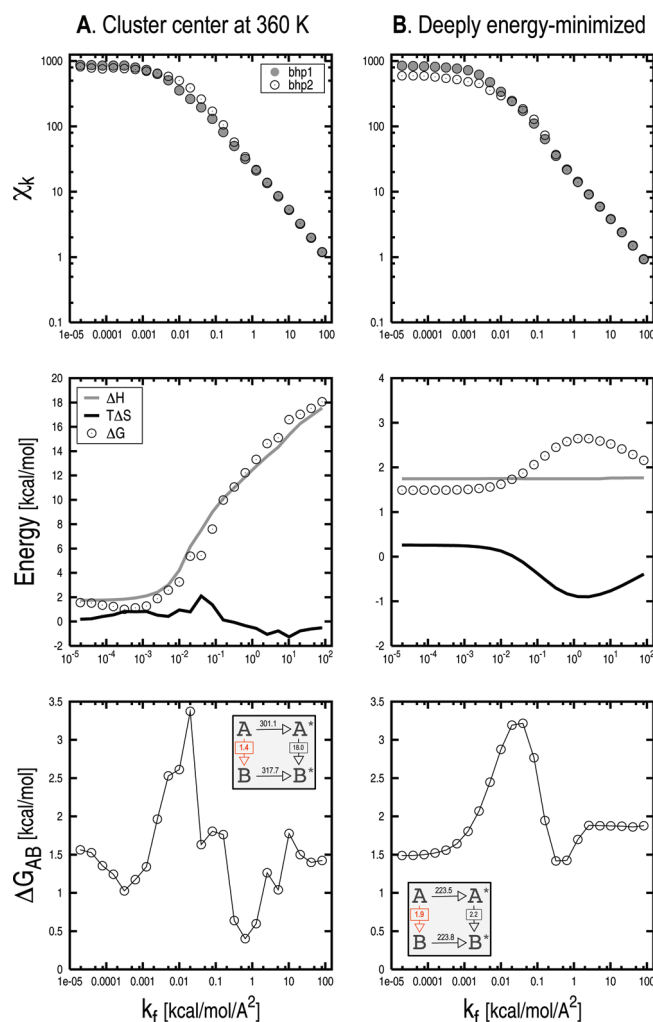


**Figure 5.** Effect of the choice of the reference structure on the confinement results for  $\beta$ -hairpin. The ensemble-averaged fluctuations ( $X_k$ ), the thermodynamic components of  $\Delta G_{A^*B^*}^{NMA}$ , and the total free-energy change (i.e.,  $\Delta G_{bhp2} - \Delta G_{bhp1}$ ) are shown at various  $k_f$  values from top to bottom, respectively. Results corresponding to different selections for the reference structure are shown: (A) the centers of the most-populated cluster at 360 K; (B) deeply energy-minimized conformations. The insets in the bottom two panels report the numerical values for the various legs of the thermodynamic cycle corresponding to a final restraint strength of 82 kcal/mol/Å<sup>2</sup>. Molecular states **A** and **B** correspond to **bhp1** and **bhp2**, respectively. The analysis indicates that energy-minimized conformations should be used as reference structures (see text).

free energy required to confine the system is larger than that required to confine it to a minimum of the PES (see below), which results in larger errors in the value of the  $\Delta G_{AB}$ .

To verify these hypotheses, the confinement calculation was repeated by selecting deeply energy-minimized conformations as reference structures. The  $X_k$  values computed at different strengths are shown in Figure 5B (top). The confinement free energies for **bhp1** and **bhp2** obtained for  $k_f = 82$  kcal/mol/Å<sup>2</sup> are equal to 223.50 and 223.78 kcal/mol, respectively. We note that the selection of energy-minimized structures as references lowers the confinement free energies for **bhp1** and **bhp2** by 77.28 and 93.9 kcal/mol, respectively. The thermodynamic cycle was finally closed by NMA, which in the presence of a restraining potential with a spring constant of 82 kcal/mol/Å<sup>2</sup> yielded a  $\Delta G^{NMA}$  of 2.16 kcal/mol ( $\Delta H^{NMA}$  and  $T\Delta S^{NMA}$  are equal to 1.76 and  $-0.40$  kcal/mol, respectively). Interestingly and in contrast to what was found above, the enthalpic



contribution to the total  $\Delta G^{\text{NMA}}$  is essentially independent of the strength of the restraining potential (Figure 5B, middle). As a result, the **bhp1/bhp2** free-energy difference shows a much smoother profile as a function of  $k_f$  and has converged to a value of 1.88 kcal/mol at  $k_f$  larger than 2 kcal/mol/Å<sup>2</sup> (Figure 5B, bottom). This value is in excellent agreement with the free-energy difference of  $1.86 \pm 0.12$  kcal/mol obtained from 200  $\mu\text{s}$  MD sampling at equilibrium; i.e., the latter was obtained from 50 independent MD simulations at 360 K each of which was 4  $\mu\text{s}$  long (see Supporting Information for details on the calculation). The comparison validates the confinement results.

**Treatment of Errors.** An understanding of the possible sources of errors in a confinement calculation is important for future applications, particularly for more complex systems. Both systematic and statistical errors that can affect the numerical value of the free-energy difference determined by the confinement method were investigated. “Systematic” errors are designated errors that are due to inaccuracies in the estimation of the ensemble-averaged fluctuations arising in the presence of strong restraining forces; the latter may cause a systematic overshooting of the potential energy minimum which leads to an overestimation of the atomic fluctuations. Systematic errors arising from inaccuracies of the potential function, which are difficult to evaluate, are not considered. If the  $\Delta G^{\text{NMA}}$  between the *confined* states of  $\beta$ -hairpin is assumed to be exact (eq 21), which is reasonable, errors result from the confinement simulations. Systematic errors are likely to occur in the high force-constant range (i.e.,  $k > 10$  kcal/mol/Å<sup>2</sup>) where too large an integration time step may lead to the above-mentioned inaccuracies in the ensemble-averaged fluctuations. By contrast, statistical errors are expected to occur in the low force-constant range (i.e.,  $0 \leq k \leq 0.001$  kcal/mol/Å<sup>2</sup>) where sampling of the essentially unconstrained basin can be intrinsically problematic. To address these issues, (i) the confinement simulations were repeated by using smaller integration time steps; and (ii) a specialized block analysis was performed to estimate the error bar on the computed  $\Delta G$  (see below).

**Systematic Errors.** To search for systematic errors, the confinement simulations in the high force-constant range (i.e.,  $k > 0.04$  kcal/mol/Å<sup>2</sup>) were repeated by decreasing the integration time step from 2.0 fs to 0.5 and 0.2 fs, i.e., 4 and 10 times smaller than the original value, respectively.  $X_k$  values were computed at different restraint strengths and confinement free energies determined as a function of  $k_f$ . As shown in Figure 6 (top), the reduction of the integration time step results in nonnegligible systematic differences in the integrated value of the free energy of confinement; i.e., up to 2.5 kcal/mol. As expected, systematic errors become important ( $>0.1$  kcal/mol) when  $k_f$  is large ( $k_f > 1$  kcal/mol/Å<sup>2</sup>). We note that for very high force constants ( $k_f > 2$  kcal/mol/Å<sup>2</sup>) nonnegligible systematic differences are found even between the 0.2 and 0.5 fs time-step results, suggesting that very short time steps are required in this range to obtain accurate free-energy values. However, despite the presence of these systematic errors,  $\Delta G_{\text{AB}}$  obtained from confinement calculations with shorter time steps are essentially the same (see Figure 6, on bottom); i.e.,  $\Delta G$  values obtained by solving eq 1 with  $k_f = 82$  kcal/mol/Å<sup>2</sup> for the 0.2, 0.5, and 2.0 fs time-step calculations are equal to 1.85, 1.87, and 1.88 kcal/mol, respectively. It is encouraging that the systematic errors in the individual confinement simulations cancel out. Our hypothesis is that for  $k_f > 2$  kcal/mol/Å<sup>2</sup> (i.e., the range in which nonnegligible systematic errors are found) the  $\beta$ -hairpin states approach the “superharmonic” region where the restraining potential is so strong that the free energy

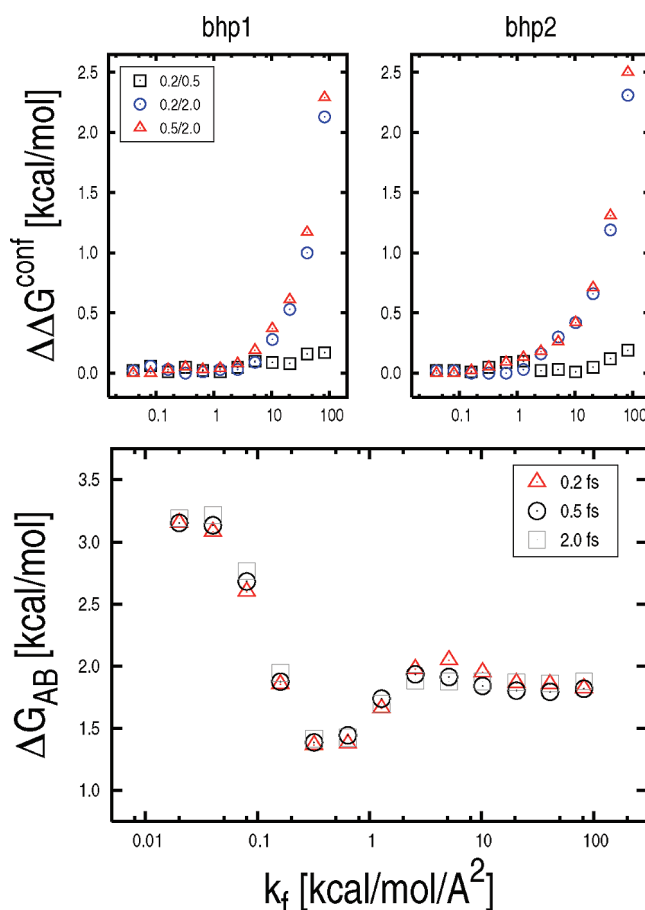


**Figure 6.** Systematic errors in the confinement calculation. On top, confinement free-energy differences determined by calculations using integration time steps of varying sizes (i.e., 2.0, 0.5, and 0.2 fs) for the  $\beta$ -hairpin states **bhp1** and **bhp2** are shown as a function of  $k_f$ . The reduction of the time-step size results in nonnegligible systematic differences. On bottom,  $\Delta G_{\text{AB}}$  (i.e.,  $\Delta G_{\text{bhp2}} - \Delta G_{\text{bhp1}}$ ) is shown as a function of  $k_f$  for the same confinement calculations. The free-energy change results are not affected by the systematic errors observed in the confinement simulations (on top).

of the harmonic oscillator becomes independent of the reference structure (see Supporting Information). This behavior, as well as the width of the superharmonic region in  $k$  space, may be system dependent and should be investigated in more detail for larger peptides and proteins.

**Statistical Errors.** Statistical errors in the confinement approach are essentially due to limited sampling in the various restrained runs. Standard analyses, such as block analysis, bootstrapping, etc., could be applied to estimate the statistical uncertainty on the ensemble-averaged fluctuations which are used to compute the free energy of confinement. However, since the individual contributions are strongly nonhomogeneous, a correct analysis would require larger weights for errors introduced in runs associated with larger contributions. Because of this complication, statistical errors were estimated by means of a specialized block analysis, which is described in the Supporting Information. Individual and cumulative statistical errors of the free energy of confinement for **bhp1** and **bhp2** are reported in Figure 7. In both cases, the largest errors are found in the intermediate  $k$  range (i.e.,  $0.001 < k < 0.3$  kcal/mol/Å<sup>2</sup>); see gray zone in Figure 7. By contrast, small errors are observed in both the high and low  $k$  ranges. The high  $k$  result is expected and consistent with the rapid convergence of the ensemble-averaged fluctuations in the presence of strong restraining

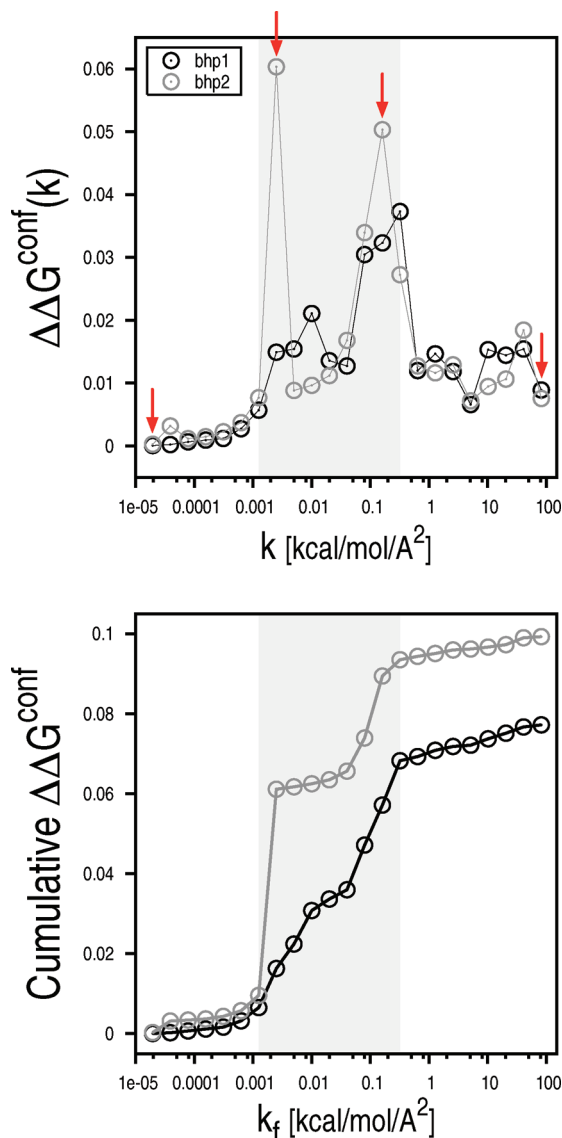


**Figure 7.** Statistical errors in the confinement calculation. Individual (top) and cumulative (bottom) statistical errors of the free energies of confinement for the  $\beta$ -hairpin states are reported as a function of  $k_f$ . Errors of the individual restrained runs were computed by dividing the MD trajectories into eight blocks. Red arrows indicate the restrained runs that were used for the free-energy profile analysis (see Figure 9). The largest statistical errors were found in the intermediate  $k$  range ( $0.001 < k < 0.3$  kcal/mol/Å<sup>2</sup>) here shown by a light-gray rectangle (see text).

potentials; the low  $k$  result is somewhat surprising. As follows from eq 15, the contributions of the individual restrained runs to the value of the free energy of confinement depend not only on the size of the ensemble-averaged fluctuations ( $X_k$ ), which are found to be larger in the low  $k$  range, but also on the strength of the restraining potential ( $k$ ) at which the fluctuations are measured. Thus, for very small values of  $k$  the confinement runs make a small, if not negligible, free-energy contribution even in the presence of large fluctuations. Analogously, statistical errors associated with these runs contribute little to the total error of the confinement free energy (see Figure 7). The analysis indicates that the confinement runs performed in the presence of restraining potentials of intermediate strength are crucial for obtaining accurate free-energy estimates.

Statistical errors of the confinement simulations were finally combined to obtain an estimate of the total error affecting the

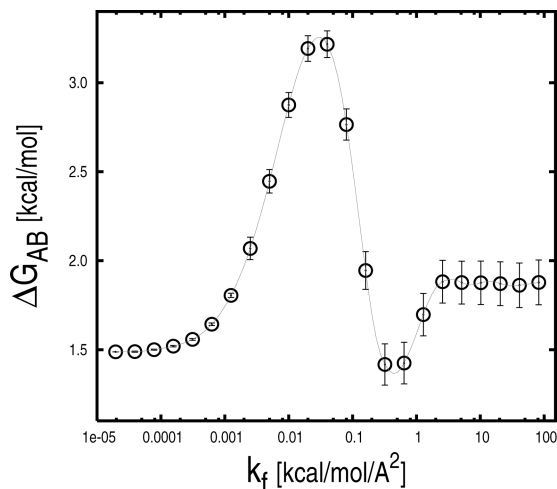


**Figure 8.** Free-energy difference between the  $\beta$ -hairpin states **bhp1** and **bhp2** (i.e.,  $\Delta G_{\text{bhp2}} - \Delta G_{\text{bhp1}}$ ).  $\Delta G_{\text{AB}}$  values along with the associated error are shown as a function of the final restraint strength,  $k_f$ . For  $k_f$  larger than 2 kcal/mol/Å<sup>2</sup>,  $\Delta G_{\text{AB}}$  has converged to a value of  $1.88 \pm 0.13$  kcal/mol.

free-energy difference determined by the confinement calculation. At 360 K, errors of the free energy of confinement for **bhp1** and **bhp2** were found to be 0.078 and 0.099 kcal/mol, respectively. Assuming  $\Delta G^{\text{NMA}}$  in eq 1 to be exact, these values were combined by the simple equation

$$\Delta\Delta G_{\text{AB}} = \sqrt{[\Delta\Delta G_{\text{AA}^*}^{\text{conf}}]^2 + [\Delta\Delta G_{\text{BB}^*}^{\text{conf}}]^2} \quad (26)$$

to account for error propagation. For  $k_f = 82$  kcal/mol/Å<sup>2</sup>,  $\Delta\Delta G_{\text{AB}}$  is equal to 0.13 kcal/mol.  $\Delta\Delta G_{\text{AB}}$  values with the associated error are shown in Figure 8 as a function of the final restraint strength,  $k_f$ . For  $k_f$  larger than 2 kcal/mol/Å<sup>2</sup>,  $\Delta\Delta G_{\text{AB}}$  has converged to a value of  $1.88 \pm 0.13$  kcal/mol.

To examine the origin of such statistical errors, the free energy was projected onto the all-atom rmsd from the reference structure for four confinement runs of **bhp2** corresponding to restraint strengths of  $1.95 \times 10^{-5}$ , 0.0025, 0.16, and 82 kcal/mol/Å<sup>2</sup> (see red arrows in Figure 7); these are the lowest and the highest  $k$  values, and the two intermediate  $k$  values that are associated with the largest errors. At all restraint strengths but the lowest, the free-energy profiles show a single basin surrounded by high barriers (see Figure 9A). This picture cannot explain the sampling problems detected in the intermediate  $k$  range so that the presence of some “hidden complexity” on the underlying free-energy surface must be introduced.<sup>31</sup> To check for that, the free energy was projected onto the “natural coordinate” resulting from a principal component analysis of the interatomic distances (see Methods). This time, the profiles corresponding to the low and intermediate restraint strengths show multiple basins separated by relatively high free-energy barriers (see Figure 9B). The latter are responsible for the large statistical errors found at intermediate  $k$  values (see Figure 7). The structural analysis of the two confinement runs at intermediate  $k$  (i.e., for  $k$  equal to 0.0025 and 0.16 kcal/mol/Å<sup>2</sup>) unveiled the origin of the hidden complexity of the free-energy landscape. The comparison of molecular snapshots extracted from basins I and II for  $k$  equal to 0.0025 kcal/mol/Å<sup>2</sup>, and basins III and V for  $k$  equal to 0.16 kcal/mol/Å<sup>2</sup> shows a striking difference in the H-bonding interaction between Thr 9 and Glu 16 (see Figure 9C). The analysis indicates that the largest barrier observed in the free-energy profiles on the “natural coordinate”

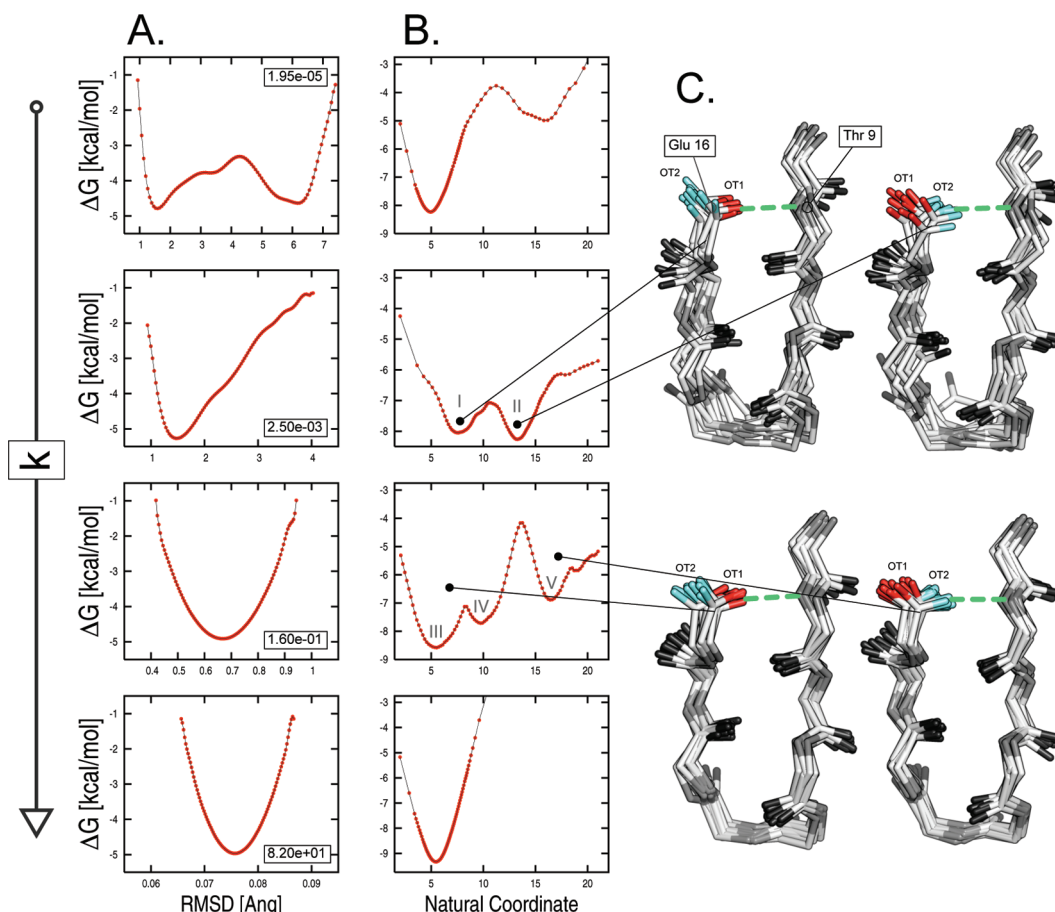


**Figure 9.** Origin of statistical errors in the confinement calculation. The analysis was carried out on a set of four restrained runs for **bhp2** with restraint strengths of  $1.95 \times 10^{-5}$ , 0.0025, 0.16, and 82 kcal/mol/Å<sup>2</sup> (from top to bottom; see insets in panel A). The free energy is projected onto (A) the all-atom rmsd from the reference structure and (B) the “natural coordinate” from a principal component analysis of the interatomic distances. The latter shows a complex landscape made of multiple basins separated by high free-energy barriers. Such complexity, which is hidden in the rmsd based free-energy profiles, is responsible for the large statistical errors found in the intermediate  $k$  range. (C) Structural analysis of two confinement runs at intermediate  $k$  values. Molecular snapshots extracted from basins I and II for  $k$  equal to 0.0025 kcal/mol/Å<sup>2</sup> (top), and basins III and V for  $k$  equal to 0.16 kcal/mol/Å<sup>2</sup> (bottom) show a striking difference in the H-bonding interaction between Thr 9 and Glu 16: the H-bond (green dashed line) involves oxygen OT1 of Glu 16 (red stick) in the former basins, and oxygen OT2 (cyan sticks) in the latter.

originates from the occurrence of permutational isomers that interconvert slowly because of H-bonding interactions (see Supporting Information for details); these isomers originate from the lack of symmetry in the calculation of the rmsd from the reference. The introduction of a specialized restraining potential that takes into account the chemical symmetry of the various amino acids is expected to remove such artifacts and increase both the accuracy and efficiency of the confinement approach (Cecchini et al. in progress).

**Definition of Free-Energy Basins.** The dependence of the confinement results on the definition of the  $\beta$ -hairpin states was investigated. The results presented above were obtained by using a cutoff of 2.0 Å in the  $C_{\alpha}$ -rmsd from the reference structures to define the boundaries of the **bhp1** and **bhp2** basins. To determine the sensitivity of the calculated free-energy difference to such an “arbitrary” definition, the analysis was repeated by using  $C_{\alpha}$ -rmsd cutoffs ranging from 1.5 to 5.0 Å. Figure 10 (top) shows that the value of the rmsd cutoff has a sizable effect on the calculated  $\Delta G_{AB}$ , but the confinement results are relatively robust for the limited range of cutoffs between 2.0 and 3.0 Å. Both too conservative or too loose criteria lead to significant changes in the results. To analyze the observed behavior, the free energies of the individual basins of  $\beta$ -hairpin were projected on the  $C_{\alpha}$ -rmsd from the reference structures for both **bhp1** and **bhp2**; i.e., the free-energy profiles shown in Figure 10 were

generated from the histograms of the  $C_{\alpha}$ -rmsd from the reference of the structural ensembles sampled by equilibrium MD at 360 K and kinetically partitioned as described in ref 31. Figure 10 shows that an approximate definition of the free-energy basins can still provide correct results if high free-energy conformations are discarded: although cutoffs of 2.0 and 3.5 Å (dashed lines in Figure 10) include rather different portions of the free-energy basins 1 and 2,  $\Delta G_{AB}$  remains unaltered in this range; i.e., the contribution of high free-energy conformations corresponding to rmsd values larger than 2.0 Å is essentially negligible. Also, “spurious” contributions coming from conformations that are erroneously assigned to the basins of interest are negligible in the range of cutoffs corresponding to stable confinement results (i.e.,  $2.0 \leq C_{\alpha}\text{-rmsd} \leq 3.5$  Å); see Figure 10 (bottom). The same is not true for cutoffs larger than 3.5 Å, where nonnegligible contributions coming from other free-energy basins are present. At the same time, cutoffs lower than 2.0 Å correspond to an incomplete description of the actual free-energy basin and lead to incorrect results as well. In particular, a cutoff of 1.5 Å results in the loss of the contribution coming from the shoulder of the free-energy profile of **bhp1**, which appears to be nonnegligible on the calculated  $\Delta G_{AB}$ .

The robustness of the confinement results relative to an approximate definition of the basins is not ensured and may be system dependent. We note that in the case of the  $\beta$ -hairpin



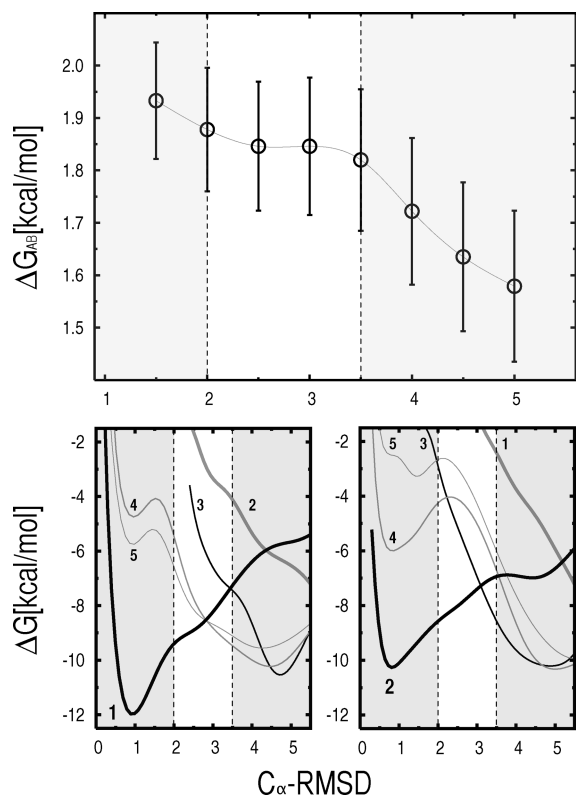


**Figure 10.** Dependence of the confinement results on the definition of the free-energy basins corresponding to the investigated molecular states. Here, the data refer to **bhp1** and **bhp2** states of the  $\beta$ -hairpin peptide. On top are shown the calculated  $\Delta G_{AB}$  values (i.e.,  $\Delta G_{bhp2} - \Delta G_{bhp1}$ ) as a function of the rmsd cutoff used in the analysis. On bottom are shown the free-energy projections of the individual basins of the  $\beta$ -hairpin peptide (see ref 31) on the  $C_{\alpha}$ -rmsd from the reference structure of both **bhp1** (left) and **bhp2** (right) states. The free-energy profiles were generated from the histograms of the  $C_{\alpha}$ -rmsd computed for each basin from the structural ensembles sampled by equilibrium MD at 360 K and kinetically partitioned as described in ref 31.

state **3**, which is structurally more heterogeneous than **bhp1** and **bhp2** because of its flexible tail, an rmsd-based definition strongly affects the free-energy results in the entire range of cutoffs (see Supporting Information for details).

## Discussion

Conformational free-energy differences are key quantities for understanding phenomena in molecular biology that involve large structural changes of macromolecules. Calculations of such free-energy differences are particularly difficult when two conformations of a macromolecule differ significantly from each other and have high barriers between them. The “confinement” approach,<sup>19</sup> which is based on early developments,<sup>21–24</sup> is a method that avoids this problem because it determines the absolute free energies of the individual states; it uses a thermodynamic cycle in which the states are progressively restrained to pure harmonic basins whose absolute free energy can be computed by normal-mode analysis. In ref 19, the confinement approach was tested on a model peptide, Met-enkephalin ( $\text{NH}_3^+ \text{-Tyr-Gly-Gly-Phe-Met-COO}^-$ ), and used to estimate side-chain entropies of a 17-residue fragment from ubiquitin.<sup>19</sup> In this paper, an improved version of the method is applied to compute the conformational free-energy difference between two states of the alanine dipeptide in vacuo, and the  $\beta$ -hairpin from protein G with an implicit treatment of the solvent. In all cases, the confinement results are found to be in

excellent agreement with the ones obtained from equilibrium molecular dynamics, while requiring a much smaller computational effort. In the case of the  $\beta$ -hairpin, for example, the confinement calculation is more efficient than equilibrium MD by a factor of 50; e.g., 4  $\mu\text{s}$  used in the confinement method and 200  $\mu\text{s}$  equilibrium MD yields comparable results. The error bars of the calculated free-energy values, given the potential energy function, are estimated to be on the order of a few tenths of a kcal/mol. Thus, the confinement method, when applied to the two systems studied here, is a technique of high accuracy and precision for computing conformational free-energy differences with relatively little computer time.

The methodological improvements presented in this paper, relative to the earlier work,<sup>19</sup> are as follows: (i) the introduction of a more convenient definition of the ensemble-averaged fluctuations from the reference structure; (ii) the use of a *best-fit* restraining potential; (iii) the introduction of a rationale for the selection of the reference structure for the confinement runs; (iv) the identification of both systematic and statistical error sources; and (v) the introduction of a quasi-harmonic analysis step as a possible approach to treating a system in explicit solvent. Each of these aspects is discussed in the following.

The ensemble-averaged atomic fluctuations from the reference ( $X_k$ ) are used to compute the free energy of confinement by numerical integration; see eqs 4 and 18. To obtain an accurate estimate of  $\Delta G_{AB}$ , it is therefore crucial to minimize the errors in the  $X_k$  values. The new definition of  $X_k$  based on the all-atom rmsd from the reference is well behaved for all restraint strengths and, unlike the one proposed in ref 19, does not diverge for vanishing  $k$ .

The newly adopted restraining potential is similar in nature to the absolute restraint described in ref 19 except that the atomic coordinates of the reference are implicitly rotated and translated so as to best fit the atoms of the actual molecular frame. Such a *best-fit* restraint minimizes the total restraint energy and does not introduce any net force or torque on the system. The former results in lower confinement free energies, thus leading to smaller errors in  $\Delta G_{AB}$ ; the latter increases the sampling efficiency. Both aspects are shown to be important for a better control of the statistical errors.

The selection of the reference structure for the confinement runs has been shown to have important effects on both the efficiency and accuracy of the method (see Figure 5). Our analysis indicates that energy-minimized molecular conformations represent the optimum choice. Their use reduces the number of restrained simulations required and minimizes the noise in the confinement results.

The occurrence of both systematic and statistical errors in the confinement results has been investigated. By varying the size of the integration time step, sizable systematic errors have been found that affect the absolute value of the confinement free energy. These errors result from nonnegligible “sampling” inaccuracies arising in the presence of large restraining forces; i.e., strong restraint strengths lead to a systematic overshooting of the potential energy minimum thus causing sizable errors on the value of the ensemble-averaged fluctuations. Nonetheless, confinement calculations applying time steps of different size yield the same  $\Delta G_{AB}$ , apparently due to error cancellation. Thus, the confinement approach appears to be robust with respect to such systematic errors and no reduction of the time-step size in the high restraint-strength range seems to be necessary to obtain accurate  $\Delta G$  values. Statistical errors were evaluated by means of a specialized block analysis designed to account for the variation in magnitude of the contributions of the individual



restrained runs to the confinement free energy. The results indicate that the confinement runs carried out in the presence of intermediate restraint strengths are the source of the largest statistical errors. In the low  $k$  range (i.e.,  $0 < k < 0.001$  kcal/mol/Å<sup>2</sup>), where sampling of the essentially unconstrained system is intrinsically problematic, the contributions of the individual runs to the free-energy of confinement are negligible because of the small  $k$  values, in spite of the large fluctuations observed. In the high  $k$  range (i.e.,  $0.3 < k < 82$  kcal/mol/Å<sup>2</sup>), the contributions to the free-energy of confinement are large, but the restraining potential is such that the fluctuations rapidly converge to their ensemble average value. The intermediate  $k$  values (i.e.,  $0.001 < k < 0.3$  kcal/mol/Å<sup>2</sup>) make the dominant contributions to  $\Delta G$ . In the intermediate  $k$  range, despite the presence of the restraining potential, the system may explore multiple subbasins separated by high free-energy barriers. These are the source of large statistical errors. The barriers are found to originate from the presence of symmetric groups (e.g., two oxygens of carboxyl groups) involved in strongly directional interactions, such as hydrogen bonds. The chemical symmetry of such groups, which has not been considered in the calculation of the restraint energy nor in the definition of the atomic fluctuations, generates "permutational isomers" (i.e., chemically equivalent but distinguishable molecular structures) that in the presence of an active restraining potential result in minima separated by free-energy barriers. Such barriers are artifacts that dramatically reduce the overall sampling efficiency. Moreover, since the multiplicity of such permutational isomers is expected to grow combinatorially with the size of the system, this problem could introduce limitations in applications of the method to biologically more relevant systems. Analogous considerations were made to circumvent the permutation problem in confinement calculations of fluid systems.<sup>54</sup> The introduction of a specialized restraining potential that removes the occurrence of permutational isomers is suggested to increase both the accuracy and efficiency of the method, while extending its scope (Cecchini et al., in progress).

An alternative version of the confinement approach has been introduced. It computes the difference in free energy between the *confined* states by a quasi-harmonic analysis instead of the normal-mode analysis. This variant requires no energy minimization and evaluates the harmonic entropy from the eigenvectors of the covariance matrix, which is directly obtained from the MD runs carried out in the presence of large restraints. The analysis showed that, as expected, the normal-mode and quasi-harmonic variants provide the same (correct) result when sufficiently strong restraining potentials are applied. However, the quasi-harmonic variant enables the analysis of a subset of degrees of freedom in a simple way and holds promise for extending the scope of the confinement method in conjunction with an explicit treatment of the solvent. In this context, one would simulate the molecular states of interest in a bath of explicit waters and apply the confinement protocol only to the protein system. Test applications of this approach are in progress and will be given separately (Cecchini et al., in progress).

Finally, the convergence rate of the conformational sampling in the confinement approach has to be considered. It has been shown that the contributions to  $\Delta G_{AB}$  of the restrained runs in the very low  $k$  range are essentially negligible, so that their convergence rate is not a concern. The largest contributions arise in the intermediate range of  $k$  (i.e.,  $0.001 < k < 1$  kcal/mol/Å<sup>2</sup>). Thus, to compute accurate estimates of  $\Delta G_{AB}$ , in the absence of permutational isomers (see above), complete sampling is required only in those confinement runs where the system

already "feels" the restraining potential and the available conformational space is limited. The latter makes the confinement method very promising for its future applications to more complex systems.

Besides the technical aspects, the present paper shows the first application of the method to the determination of full conformational free-energy differences for a realistic polypeptide system, i.e., the  $\beta$ -hairpin of protein G. The data presented here indicate that accurate predictions can be obtained at an affordable CPU cost; i.e., the analysis of a 4  $\mu$ s MD trajectory with an identical simulation setup<sup>31</sup> underestimated the conformational  $\Delta G$  between **bhp1** and **bhp2** by about 1 kcal/mol, as confirmed by the analysis of a 200  $\mu$ s MD run (see Supporting Information). It should be noted, however, that the results depend on the definition of the free-energy basins, which are used to select conformations representative of the investigated molecular states. For the  $\beta$ -hairpin states **1** and **2** it has been shown that an operational definition of the free-energy basin making use of an arbitrary cutoff on the  $C_{\alpha}$ -rmsd from the reference can provide correct results and that the confinement predictions are robust over a wide range of cutoffs. This is not the case for the structurally more heterogeneous state **3** for which an rmsd-based definition of the basin strongly affects the free-energy results in the entire range of cutoffs. This behavior suggests that the analysis of the free-energy trend over a range of cutoffs can be used for judging the quality of the confinement results. In this respect, we note that all methods for calculating free energies of different conformations will suffer from an inherent arbitrariness in the definition of the molecular states.

The results presented in this paper indicate that the confinement approach is a powerful technique for the accurate determination of conformational free-energy difference at a reasonable CPU cost. Even though its predictive power has to be further tested on systems of greater complexity for which sampling can be inherently problematic, the approach has the potential of becoming a useful tool for the efficient estimation of the free-energy difference between the conformations of a macromolecule.

**Acknowledgment.** The computations were done in part on an IBM SP6 machine at the Institut du Développement et des Ressources en Informatique Scientifique in Orsay and in part on an IBM SP4 machine at the Centre Informatique National de l'Enseignement Supérieur in Montpellier. The analysis was performed on a Beowulf cluster running Linux in Strasbourg and we thank F. Rao for setting up and maintaining the cluster. The research done at Harvard was supported in part by a grant from the National Institutes of Health (USA) and that in Strasbourg by the Centre National de la Recherche Scientifique (France). M.C. and S.K. were supported by a grant from the Human Frontier Science Program. M.C. also received partial support from the Swiss National Science Foundation (Grant No. PBZHA-112715).

**Supporting Information Available:** Free-energy differences obtained from equilibrium MD sampling for the alanine dipeptide and the  $\beta$ -hairpin with an implicit treatment of the solvent; analysis of the thermodynamic components of the free energy of confinement for the alanine dipeptide; the calculation of  $\Delta G^{NMA}$  in the quantum-mechanical framework; the description of the specialized block analysis used to estimate the statistical error of the confinement free energy; the confinement analysis of the out-of-register  $\beta$ -hairpin state (**bhp3**). This material is available free of charge via the Internet at <http://pubs.acs.org>.

## References and Notes

- (1) Karplus, M.; Gao, Y. Biomolecular motors: the F1-ATPase paradigm. *Curr. Opin. Struct. Biol.* **2004**, *14* (2), 250–259.
- (2) Hammes, G. Mechanism of enzyme catalysis. *Nature* **1964**, *204* (4956), 342–343.
- (3) Gavish, B.; Werber, M. Viscosity-dependent structural fluctuations in enzyme catalysis. *Biochemistry* **1979**, *18*, 1269–1275.
- (4) Geeves, M.; Holmes, K. Structural mechanism of muscle contraction. *Annu. Rev. Biochem.* **1999**, *68*, 687–727.
- (5) Geeves, M.; Holmes, K. The molecular mechanism of muscle contraction. *Adv. Protein Chem.* **2005**, *71*, 161–193.
- (6) Edelstein, S.; Lena, C.; Le Novère, N.; Marubio, L. Brain nicotinic receptors: structure and regulation, role in learning and reinforcement. *Brain Res. Rev.* **1998**, *26*, 198–216.
- (7) Taly, A.; Corringer, P. J.; Grutter, T.; de Carvalho, L. P.; Karplus, M.; Changeux, J. P. Implications of the quaternary twist allosteric model for the physiology and pathology of nicotinic acetylcholine receptors. *Proc. Natl. Acad. Sci. U.S.A.* **2006**, *103* (45), 16965.
- (8) Hardy, J.; Wells, J. Searching for new allosteric sites in enzymes. *Curr. Opin. Struct. Biol.* **2004**, *14* (6), 706–715.
- (9) Cui, Q.; Karplus, M. Allosteric and cooperativity revisited. *Protein Sci.* **2008**, *17* (8), 1295–1307.
- (10) Boehr, D. D.; McElheny, D.; Dyson, H. J.; Wright, P. E. The Dynamic Energy Landscape of Dihydrofolate Reductase Catalysis. *Science* **2006**, *313* (5793), 1638.
- (11) Henzler-Wildman, K.; Lei, M.; Thai, V.; Kerns, S.; Karplus, M.; Kern, D. A hierarchy of timescales in protein dynamics is linked to enzyme catalysis. *Nature* **2007**, *450* (7171), 913.
- (12) Kirkwood, J. G. Statistical mechanics of fluid mixtures. *J. Chem. Phys.* **1935**, *3*, 300.
- (13) Zwanzig, R. High-temperature equation of state by a perturbation method. i. nonpolar gases. *J. Chem. Phys.* **1954**, *22*, 1420–1426.
- (14) Archontis, G.; Simonson, T.; Karplus, M. Binding free energies and free energy components from molecular dynamics and Poisson-Boltzmann calculations. Application to amino acid recognition by aspartyl-tRNA synthetase. *J. Mol. Biol.* **2001**, *306* (2), 307–327.
- (15) Shirts, M.; Pitner, J.; Swope, W.; Pande, V. Extremely precise free energy calculations of amino acid side chain analogs: Comparison of common molecular mechanics force fields for proteins. *J. Chem. Phys.* **2003**, *119*, 5740.
- (16) Pearlman, D.; Kollman, P. The lag between the Hamiltonian and the system configuration in free energy perturbation calculations. *J. Chem. Phys.* **1989**, *91*, 7831.
- (17) Elber, R. Long-timescale simulation methods. *Curr. Opin. Struct. Biol.* **2005**, *15* (2), 151–156.
- (18) Meirovitch, H. Recent developments in methodologies for calculating the entropy and free energy of biological systems by computer simulation. *Curr. Opin. Struct. Biol.* **2007**, *17* (2), 181–186.
- (19) Tyka, M.; Clarke, A.; Sessions, R. An Efficient, Path-Independent Method for Free-Energy Calculations. *J. Phys. Chem. B* **2006**, *110*, 17212–17220.
- (20) Ytreberg, F.; Zuckerman, D. Simple estimation of absolute free energies for biomolecules. *J. Chem. Phys.* **2006**, *124*, 104105.
- (21) Hoover, W.; Gray, S.; Johnson, K. Thermodynamic Properties of the Fluid and Solid Phases for Inverse Power Potentials. *J. Chem. Phys.* **1971**, *55*, 1128.
- (22) Frenkel, D.; Ladd, A. New Monte Carlo method to compute the free energy of Arbitrary solids. Application to the fcc and hcp phases of hard spheres. *J. Chem. Phys.* **1984**, *81*, 3188.
- (23) Singer, K. The molar free energy of solids. *CCP5 Newslett.* **1986**, *22*, 1–4.
- (24) Stoessel, J.; Nowak, P. Absolute free energies in biomolecular systems. *Macromolecules* **1990**, *23* (7), 1961–1965.
- (25) Park, S.; Lau, A.; Roux, B. Computing conformational free energy by deactivated morphing. *J. Chem. Phys.* **2008**, *129*, 134102.
- (26) Zheng, L.; Chen, M.; Yang, W. Random walk in orthogonal space to achieve efficient free-energy simulation of complex systems. *Proc. Natl. Acad. Sci.* **2008**, *105* (51), 20227.
- (27) Maragakis, P.; Spichty, M.; Karplus, M. A Differential Fluctuation Theorem. *J. Phys. Chem. B* **2008**, *112*, 6168.
- (28) Brooks, B. R.; Karplus, M. Harmonic dynamics of proteins: Normal modes and fluctuations in bovine pancreatic trypsin inhibitor. *Proc. Natl. Acad. Sci. U.S.A.* **1983**, *80*, 6571–6575.
- (29) Case, D. Normal-mode analysis of protein dynamics. *Curr. Opin. Struct. Biol.* **1994**, *4*, 285–290.
- (30) Brooks, B. R.; Janežic, D.; Karplus, M. Harmonic analysis of large systems. i. methodology. *J. Comput. Chem.* **1995**, *16*, 1522–1542.
- (31) Krivov, S.; Karplus, M. Hidden complexity of free energy surfaces for peptide (protein) folding. *Proc. Natl. Acad. Sci. U.S.A.* **2004**, *101*, (41), 14766.
- (32) Beveridge, D. L.; DiCapua, F. M. Free energy via molecular simulation; a primer. In *Computer simulation of biomolecular systems*; van Gunsteren, W. F., Weiner, P. K., Eds.; Springer: New York, 1989; pp 1–26.
- (33) McQuarrie, D. A. *Statistical mechanics*; Harper and Row: New York, 1976.
- (34) Brooks, B.; Brucoleri, R.; Olafson, B.; States, D.; Swaminathan, S.; Karplus, M. CHARMM: A program for macromolecular energy, minimization, and dynamics calculations. *J. Comput. Chem.* **1983**, *4*, 187–217.
- (35) Karplus, M.; Kushick, J. Method for estimating the configurational entropy of macromolecules. *Macromolecules* **1981**, *14*, 325–332.
- (36) Levy, R.; Karplus, M.; Kushick, J.; Perahia, D. Evaluation of the configurational entropy for proteins: application to molecular dynamics simulations of an  $\alpha$ -helix. *Macromolecules* **1984**, *17*, 1370–1374.
- (37) Krivov, S.; Karplus, M. One-Dimensional Free-Energy Profiles of Complex Systems: Progress Variables that Preserve the Barriers. *J. Phys. Chem. B* **2006**, *110*, 12689.
- (38) Krivov, S.; Muff, S.; Caffisch, A.; Karplus, M. One-Dimensional Barrier-Preserving Free-Energy Projections of a  $\beta$ -sheet Miniprotein: New Insights into the Folding Process. *J. Phys. Chem. B* **2008**, *112*, 8701–8714.
- (39) Krivov, S.; Karplus, M. Diffusive reaction dynamics on invariant free energy profiles. *Proc. Natl. Acad. Sci.* **2008**, *105* (37), 13841.
- (40) Elmáci, N.; Berry, R. Principal coordinate analysis on a protein model. *J. Chem. Phys.* **1999**, *110*, 10606.
- (41) Rao, F.; Caffisch, A. The Protein Folding Network. *J. Mol. Biol.* **2004**, *342* (1), 299–306.
- (42) Olender, R.; Elber, R. Calculation of classical trajectories with a very large time step: Formalism and numerical examples. *J. Chem. Phys.* **1996**, *105*, 9299.
- (43) Smith, P. The alanine dipeptide free energy surface in solution. *J. Chem. Phys.* **1999**, *111*, 5568.
- (44) Mackerell, A.; Feig, M.; Brooks, C. Extending the treatment of backbone energetics in protein force fields: Limitations of gas-phase quantum mechanics in reproducing protein conformational distributions in molecular dynamics simulations. *J. Comput. Chem.* **2004**, *25* (11), 1400–1415.
- (45) Ren, W.; Vanden-Eijnden, E.; Maragakis, P.; Weinan, E. Transition pathways in complex systems: Application of the finite-temperature string method to the alanine dipeptide. *J. Chem. Phys.* **2005**, *123*, 134109.
- (46) van der Vaart, A.; Karplus, M. Simulation of conformational transitions by the restricted perturbation-targeted molecular dynamics method. *J. Chem. Phys.* **2005**, *122*, 114903.
- (47) Gronenborn, A.; Filpula, D.; Essig, N.; Achari, A.; Whitlow, M.; Wingfield, P.; Clore, G. A novel, highly stable fold of the immunoglobulin binding domain of streptococcal protein G. *Science* **1991**, *253* (5020), 657–661.
- (48) Neria, E.; Fischer, S.; Karplus, M. Simulation of activation free energies in molecular systems. *J. Chem. Phys.* **1996**, *105*, 1902–1921.
- (49) Apostolakis, J.; Ferrara, P.; Caffisch, A. Calculation of conformational transitions and barriers in solvated systems: Application to the alanine dipeptide in water. *J. Chem. Phys.* **1999**, *110*, 2099–2108.
- (50) Lazaridis, T.; Karplus, M. Effective energy function for proteins in solution. *Proteins: Struct. Funct. Genet.* **1999**, *35*, 133–152.
- (51) Ryckaert, J. P.; Cicciotti, G.; Berendsen, H. J. C. Numerical integration of the Cartesian equation of motion of a system with constraints: Molecular dynamics of n-alkanes. *J. Comput. Phys.* **1977**, *23*, 327–341.
- (52) Seeber, M.; Cecchini, M.; Rao, F.; Settanni, G.; Caffisch, A. Wordom: a program for efficient analysis of molecular dynamics simulations. *Bioinformatics* **2007**, *23*, 2625–2627.
- (53) Sugita, Y.; Okamoto, Y. Replica-exchange molecular dynamics method for protein folding. *Chem. Phys. Lett.* **1999**, *314*, 141–151.
- (54) Tyka, M.; Sessions, R.; Clarke, A. Absolute Free-Energy Calculations of Liquids Using a Harmonic Reference State. *J. Phys. Chem. B* **2007**, *111*, 9571.
- (55) DeLano, W. *The PyMOL Molecular Graphics System*; DeLano Scientific: San Carlos, CA, 2002.